Angular distribution of laser-ablated species from a $Pr_{0.67}Sr_{0.33}MnO_3$ target

Haijun Dang and Qizong Qin*
Laser Chemistry Institute, Fudan University, Shanghai 200433, People's Republic of China
(Received 13 January 1999)

The angular distributions of laser ablated species generated from a colossal magnetoresistant metal-oxide $Pr_{0.67}Sr_{0.33}MnO_3$ at 532 and 355 nm have been investigated by an angle- and time-resolved quadrupole mass spectrometric technique. It is found that the angular distributions of ionic and neutral ablated species vary distinctly with respect to the kinds of the ablated species as well as the laser fluence. For the laser ablation of a dense target at a moderate fluence, the angular distributions of the ablated species can be described by a $\cos^n\theta$ or a bicosine function $a\cos\theta+(1-a)\cos^n\theta$. [S0163-1829(99)04439-2]

I. INTRODUCTION

As a powerful and universal film deposition technique, pulsed laser deposition (PLD) has been drawing much attention in the recent decade. Thin films of high-T_c superconductor $YBa_2Cu_3O_{7-\delta}$ and colossal-magnetoresistant (CMR) divalent metal doped lanthanide magnites, such as $La_{1-x}Ca_xMnO_3$ and $Pr_{1-x}Sr_xMnO_3$ as well as dielectric Ta_2O_5 and TiO_2, have been fabricated successfully by the PLD method.[1–4] In order to facilitate the development and improvement of a PLD process, various techniques including time-of-flight quadrupole mass spectroscopic analysis[5–7] and optical diagnosis[8,9] have been employed to examine the underlying mechanism of laser ablation. It is well known that the quality of pulsed laser deposited thin films is closely related to the composition of the laser ablated plume, as well as the velocity and angular distribution of the ablated species.[10]

Angular distribution of laser ablated species provides much instructive information about the ablation mechanism as it is closely related to the expansion dynamics of the ablated plume, and hence, in some senses, affects the film uniformity in both its chemical composition and thickness. Since the success of the laser deposition of high-T_c superconductive films in late 80s, great efforts have been carried out to clarify the nature and the behavior of angular distribution of ablated species. Two methods of examination of the angular distributions have been employed, one is the measurement of the radial thickness distribution of the deposited film, and the other is the direct determination of the angular dependence of the ejection flux of ablated species. A great deal of studies have been reviewed by Saenger concerning the angular distributions of ablated species,[11] and it was found that although a great variety has been observed in the angular distributions of laser ablated species from metal oxides, generally, $\cos^n\theta$ and/or a bicosine function $a\cos\theta+(1-a)\cos^n\theta$ are usually employed to describe the angular distributions of ablated species. Venkatesan *et al.* have studied the deposition of Y-Ba-Cu-O film and suggested that the angular distribution consists of two distinct components,[12] one is a broad component resulting from a thermal evaporation process induced by the laser heating of the target surface, which obeys a $\cos\theta$ distribution (Knudsen law), while the other is a forward-directed component undergoing a second ejection due to the collisions between the ablated species, which has a sharp angle dependence and can be described by a $\cos^n\theta\,(n>1)$ distribution, where n is the sharpness parameter. Hansen, Schcu, and Lunney have studied the angular distribution of laser ablated Ag^+ and found that the forward-directed component mainly consist of Ag^+ ions.[13] Schreiner and Urbassek have demonstrated by theoretical simulation that fast species does not account for the nonthermal $\cos^n\theta$ term in the angular distribution; on the contrary, fast species broadens the angular distribution.[14] But whatever the mechanisms of these two components might be, $\cos\theta$ and/or $\cos^n\theta$ are valid for most experimental cases. Qin, Han, and Dang have studied the laser ablation of Ta_2O_5 and found that the ablated ions are ejected strongly forward-peaked while the ablated neutrals are regulated by Knudsen law, which follows a $\cos\theta$-type angular distribution.[6] However, despite the great efforts to understand the PLD technique, the nature of laser ablation has not been made very clear and the mechanisms underlying the angular distributions are still controversial. In this paper, we employ an angle- and time-resolved mass spectrometric technique to study the angular distributions of ablated species from a CMR Pr-Sr-Mn-O target as well as the laser fluence effects. The angle dependence of the kinetic energy of ablated species is also examined. By these measurements we try to gain insight of the ablation mechanism.

II. EXPERIMENT

The experimental apparatus used in this work has been described previously.[6] Briefly, a reaction chamber was pumped down to a base pressure of $\sim 10^{-6}$ torr. A $Pr_{0.67}Sr_{0.33}MnO_3$ disc target was mounted onto a rotatable target holder, which was fixed at the center of the chamber. The ablated species were measured by a quadrupole mass spectrometer (QMS, ULVAC MSQ-400) housed in the detection chamber, which was designed to be able to move around the laser beam-target interaction center for a range of $0\sim 90°$. The time-of-flight spectra were recorded with a 10-MHz transient recorder, which was interfaced to a computer and triggered synchronously by the laser pulses. Ionic species were detected with the ionizer of QMS switched off. When the ionizer was switched on, the overall ions, including the nascent ionic ablated species and the ions originated

from electron impact ionization of the neutrals by 70 eV electrons in the ionizer were recorded.

The 355 and 532 nm laser beams, with a pulse width of 6 ns and a repetition rate of 10 Hz, were provided by the third and second harmonic frequencies of a *Q*-switched Nd:YAG laser (Quanta Ray GCR-190). The laser beam was focused onto the target surface at an incident angle of 45° with respect to the surface normal. The diameter of the laser spot was about 0.75 mm and the laser intensity was measured with an Ophir DG-HH power meter.

The $Pr_{0.67}Sr_{0.33}MnO_3$ (simply noted as Pr-Sr-Mn-O) disc target was prepared by successive sintering, grinding, and pressing[2] and proved to be colossal magnetoresistant as prepared.

III. RESULTS AND DISCUSSION

A. The mechanism of angular distribution

It is well known that a great amount of ablated species will be ejected within a very short time when a pulsed laser beam irradiates a solid target surface. These species with a great density in the ablated plume might collide with each other and are directed toward the surface normal. The origin of angular distribution lies in the fact that the initial velocity distribution of the ablated species is a half Maxwell-Boltzmann distribution ($v_z \geqslant 0$, where **z** denotes the direction normal to the target surface). It can be illustrated as follows: As the symmetry of the ablated plume in **x** and **y** directions which define a plane parallel to the target surface, its partial momentum p_x and $p_y = 0$, while $p_z \geqslant 0$. Let the initial velocity of a certain particle i is v_{i0} with the velocity component in **z** direction of v_{zi0}, then its initial projectile angle

$$\theta_0 = \arccos(v_{zi0}/v_{i0}), \tag{1}$$

After a serious of elastic and inelastic collisions between the ablated species, the velocity and the component in z direction of the particle become v_i and v_{zi} when it enters the free-flight region in vacuum, then the ejection angle

$$\theta = \arccos(v_{zi}/v_i). \tag{2}$$

Due to the momentum conservation, v_{zi} is expected to be equal to v_{zi0}, while v_i is expected to be less than v_{i0} taking into account the kinetic energy loss in collisions. So each particle is expected to be deflected toward the surface normal during the collisions, i.e., $\theta < \theta_0$. On the other hand, as the expansion is much greater in **z** direction than in the **x**-**y** plane, the initial inner energy of the plume is converted into kinetic energy mostly in **z** direction rather than in **x**-**y** plane. These mechanisms both contribute to the narrowing of the angular distribution. It is clear that the expansion of the plume also tailors the velocity distribution of ablated species, so one might expect an intrinsic relation between the angular distribution and the velocity distribution of the ablated species.

In fact, the well accepted angular distribution $\cos^n\theta$ is a good approximation of what is derived from the velocity distribution of ablated species. In a real-ablation system, due to the surface escape barrier, a particle with a greater v_z may have greater escape probability, so following velocity distribution is usually recommended for the ablated species:

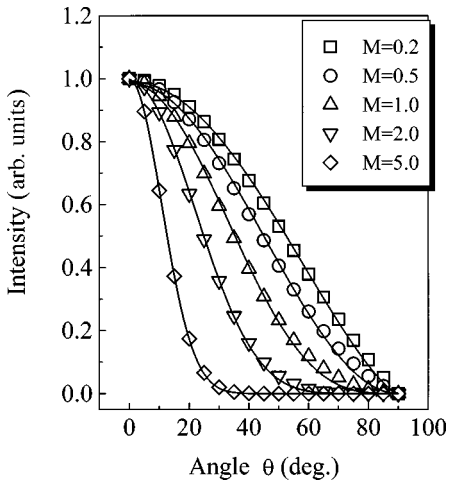

FIG. 1. The predicted angular distributions of laser ablated species (solid lines are fitted curves with $\cos^n\theta$), M is the apparent Mach number defined by $M = u/v_0 = u(2kT/m)^{-1/2}$.

$$f(v_x, v_y, v_z)\,dv_x\,dv_y\,dv_z = C v_z e^{-(m/2kT)[v_x^2 + v_y^2 + (v_z - u)^2]}\,dv_x\,dv_y\,dv_z, \tag{3}$$

Transforming into a global coordination system, it becomes

$$f(v,\Omega)\,d\Omega\,dv = C v^3 \cos\theta e^{-(m/2kT)[v^2 \sin^2\theta + (v\cos\theta - u)^2]}\,d\Omega\,dv, \tag{4}$$

where Ω is the solid angle, v is the velocity of the species, θ is the ejection angle with respect to the surface normal, m is the mass, T is a temperature parameter, u is the stream velocity, and k is Boltzmann constant. Integrating $f(v,\Omega)$ over v gives the angular distribution. It should be noted that the exact analytical integration is impossible. However, kinds of approximation have been employed to give an empirical formula, among them the following equation can give a perfect reproduction of the exact solution:[11,15]

$$f(\theta) = B\cos\theta e^{-M^2\sin^2\theta} \cdot \sum_{i=0}^{3} a_i (M\cos\theta)^i, \tag{5}$$

where $a_0 = 0.5$, $a_1 = 1.8$, $a_2 = 0.25$, and $a_3 = \pi^{1/2}$. $M = u/v_0$ is the apparent Mach number with $v_0 = (2kT/m)^{1/2}$ being the thermal velocity. It is clear that Eq. (5) can degenerates to reproduce the $\cos\theta$ form for thermal evaporation when u is zero. Detailed analysis shows that each term and the overall can all be approximated by $\cos^p\theta$. It means that Eq. (5) can be well reproduced with the following equation:

$$f(\theta) = A_1\cos^{p1}\theta + A_2\cos^{p2}\theta + A_3\cos^{p3}\theta + A_4\cos^{p4}\theta \approx \cos^p\theta, \tag{6}$$

A_i and p_i ($i = 1$ to 4) are parameters as functions of Mach number. Figure 1 shows the results from Eq. (5) and fittings with Eq. (6), and the fitted parameters are listed in Table I. The following relation between p and M can be concluded:

$$p = 1.05 + 1.40M + 0.81M^2. \tag{7}$$

In laser ablation process, the velocity of ablated species is usually described by a bicomponent Maxwell-Boltzmann

TABLE I. The fitted parameters for different Mach number.

$M=u/v_0$	p_1	p_2	p_3	p_4	p
0.0	/	/	/	/	1
0.2	1.025±0.002	2.030±0.002	3.033±0.001	4.034±0.001	1.38±0.01
0.5	1.16±0.01	2.19±0.01	3.21±0.01	4.21±0.01	1.96±0.04
1.0	1.72±0.03	2.80±0.02	3.84±0.02	4.87±0.02	3.34±0.06
2.0	4.43±0.08	5.54±0.07	6.61±0.06	7.65±0.05	7.03±0.07
5.0	25.3±0.10	26.3±0.10	27.4±0.09	28.4±0.09	28.3±0.09

(MB) distribution due to either the different formation mechanisms or the plume splitting during expansion.[16] Usually the fast component is characterized by a sharp velocity distribution, which implies a great stream velocity while the slow component by a broad velocity distribution, typically a MB distribution with zero stream velocity. From the above discussion, we know that the angular distribution should be described by a two-component function, namely a bicosine function $a\cos\theta+(1-a)\cos^n\theta$ in this case.

B. Angular distributions of ablated species

The time-of-flight (TOF) spectra of ablated species at a laser fluence of 1.8 J/cm^2 ejected from a Pr-Sr-Mn-O target were recorded at different detection angle. Figure 2 displays the angle-dependent TOF spectra of 355-nm laser ablated species measured at $m/e55\,(Mn^+)$ with the ionizer of QMS switched off (a) and on (b), respectively. It is seen that the TOF spectra show only one component peaking at $\sim$40 μs when the ionizer of the QMS is switched off, and the peak intensity and the integrated signal intensity fall dramatically with the increase of the detection angle. When the ionizer is switched on, however, the measured TOF spectra consist of two components, a fast one corresponding to the nascent ionic Mn^+ and a slow one corresponding to neutral Mn. The fast component has the same peak time and similar peak shape as the measured with the ionizer switched off. The bicomponent spectra as shown in Fig. 2(b) can be fitted with a bicomponent shifted Maxwell-Boltzmann (MB) velocity distribution,[17] and by fitting, the peak times and integrated intensities for both components of Mn^+ can be found.

The relative flux of the ablated species is obtained by integrating the corresponding TOF spectra, taking into consideration the velocity dependence of the detection efficiency of QMS. The plot of the flux versus the detection angle gives the angular distribution. In Fig. 3, angular distributions of laser ablated nascent Mn^+ and neutral Mn are presented for the data in Fig. 2. It is found that the ablated ionic species are strongly directed to the surface normal while the neutral species has a quite different angular distribution, in which there is a broader peak along with a slowly varying component dominated at large detection angle.

From our simulation results of the angular distribution for both ionic and neutral Mn, the bicosine equation $a\cos\theta+(1-a)\cos^n\theta$ with $a=0.28$ and $n=16$ gives a satisfactory fitting for the neutral Mn, while a one-term $\cos^n\theta$ cannot fit the angular distribution of nascent Mn^+ so well. Instead, it also needs the bicosine equation with $a=0.1$ and $n=107$. It means that both the ablated ions and the neutrals originate from thermal evaporation and nonthermal ejection mechanism. Integrating the above bicosine equation $a\cos\theta+(1-a)\cos^n\theta$ over the hemispherical space results in the contribution fraction of thermal process,[18] i.e.,

$$f=\frac{na+a}{an-a+2}. \tag{8}$$

It is estimated that the thermal process contributes not only to the neutral Mn production by 77%, but also to the ionized Mn^+ production by 86%. The nonthermal part of neutral production may concern the ion-electron combination and the nonemitting decay of excited species, while the thermal contribution of ions (the $\cos\theta$ term) may come from those ablated ions at the relatively low-density wings of the expansion as well as those at the leading and trailing edges of the pulse which, suffering fewer collisions and thus having a more ''effusivelike'' velocity distribution, will contribute to the broadened distribution.[15] This isotropic ejection profile was also observed in ablation of metal target such as Cu (Ref. 19) and was attributed to a so-called ''Coulomb explosion.'' In a laser ablation, the generated electrons have much greater velocity than the positive ions and escape the plume shortly after production, leaving the position ions behind. Thus, a positively charged vapor cloud can be formed and the coulomb repel between the charged particles forces them escape from each other isotropically, and an isotropic component is overridden on the forward-directed component in angular distribution.

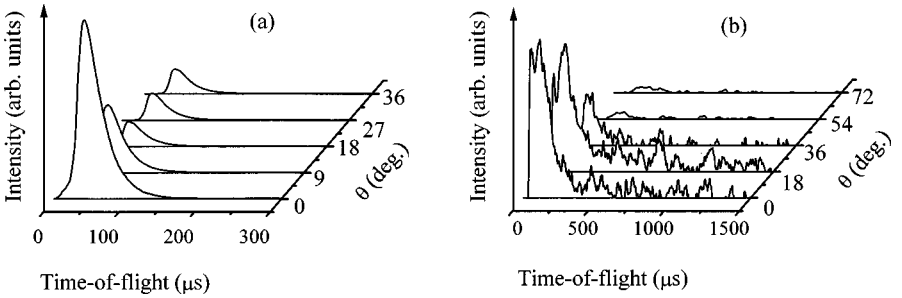

FIG. 2. Time-of-flight spectra of Mn^+ ($m/e=55$) measured at a different detection angle θ at a laser fluence of 1.8 J/cm^2. (a) ionizer off, (b) Ionizer on.

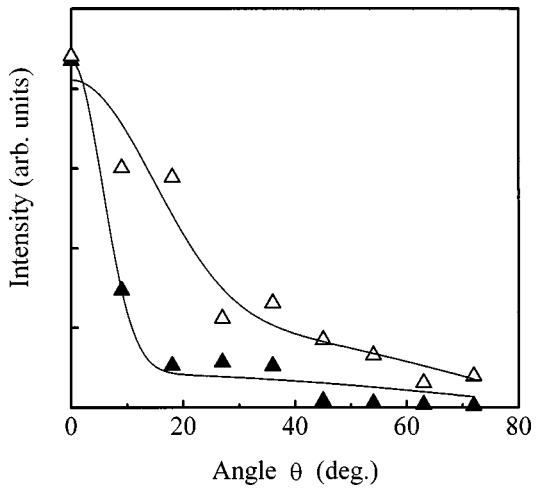

FIG. 3. Angular distributions of ablated Mn^+ (▲) and Mn (△) from a 532-nm laser ablation of a Pr-Sr-Mn-O target at a laser fluence of 1.8 J/cm.^{2}

The angular distributions of Mn^+, Sr^+, and Pr^+ ablated at 355 nm at 1.2 J/cm^2 is presented in Fig. 4 and good $\cos^n\theta$ fittings are shown with $n=8$, 5, and 9, respectively. As an example for 532-nm laser ablation, angular distributions of oxide species PrO and Mn ablated at 1.5 J/cm^2 are shown in Fig. 5, the fitted n for $\cos^n\theta$ is 3 and 7, respectively.

From the MB fitting of the measured TOF spectra, the stream velocity of ablated species are found to be 1.9×10^3, 2.3×10^3, and 1.7×10^3 m/s for Mn^+, Sr^+, and Pr^+, respectively, while the thermal motion velocity are found to be 2.8×10^3, 2.0×10^3, and 1.5×10^3 m/s, respectively. The apparent Mach number is then calculated to be 0.7, 1.15, and 1.13, respectively. The p value in Eq. (7) is estimated to be 2.5, 3.7, and 3.6, deviated from the measured n. This suggests that other narrowing mechanism such as activated ejection may also account for the measured angular distribution.

As for PLD technique, the angular distributions of the ablated species affect the film quality and the homogeneity of the relative concentration of each constitute. From the measured angular distributions shown in Figs. 4 and 5, it is clear that different ablated species share a similar angular

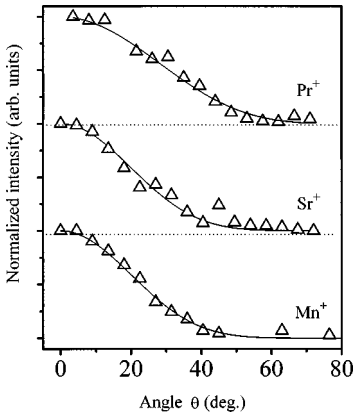

FIG. 4. Angular distributions of ionic species Mn^+, Sr^+, and Pr^+ from a 355-nm laser ablation of a Pr-Sr-Mn-O target at a laser fluence of 1.2 J/cm.^{2}

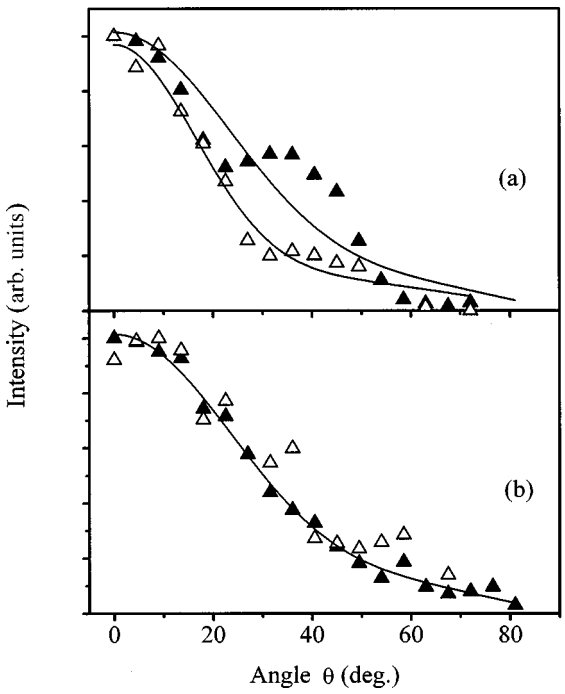

FIG. 5. Angular distributions of PrO (a) and Mn (b) from a 532-nm laser ablation of a Pr-Sr-Mn-O target at a laser fluence of 1.5 J/cm.^{2} (▲: ionizer off, △: ionizer on).

distribution in a same ablation process. In Fig. 6, we plot the relative intensity of Sr^+, Pr^+, and PrO^+ normalized to Mn^+. It can be seen that these main ablated species are ejected almost with a constant stoichiometry within the angle of 20°. Similar conclusions can be drawn for the neutral species. This demonstrates that the composition of deposited films can be expected to be uniform along the film surface for a typical arrangement of PLD process.

C. Angle dependence of the kinetic energy of ablated species

As we have mentioned above, the velocity and the kinetic energy of the ablated species can be estimated from their TOF spectra measured. In Fig. 7, the peak times (a) and corresponding kinetic energies (b) of the nascent Mn^+ and neutral Mn are presented as a function of the detection angle. It is clear that the peak time of the nascent Mn^+ keeps constant while that of the neutral Mn is steadily delayed with increasing the detection angle. It is interesting that the kinetic energy of the neutral Mn decreases by several folds

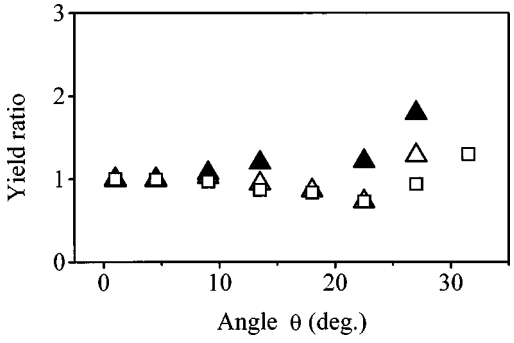

FIG. 6. The ratios of ablation yield Sr^+/Mn^+ (△), Pr^+/Mn^+ (▲) and PrO^+/Mn^+ (□) as a function of the detection angle.

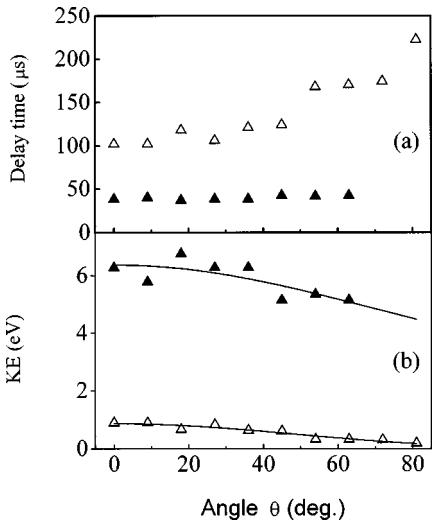

FIG. 7. The delay times (a) and kinetic energy (b) of ablated Mn^+ (▲) and Mn (△) as a function of the detection angle.

when the detection angle varies from 0° to 80°, but the absolute decrease in kinetic energy is nearly the same as that of nascent Mn^+. Previous studies on laser-induced etching of metal showed that the kinetic energy of the desorbed species from a hot surface decreases distinctly with increasing the detection angle,[17] so it might be reasonable to attribute the neutral ablated species to the thermal evaporation mechanism. However, although either $\cos^n\theta$ or $a\cos\theta+(1-a)\cos^n\theta$ fitting can be explained from the velocity distribution, the angle dependence of the kinetic energy of ablated species deviates greatly from what may be expected. From Eq. (4), the kinetic energy (E_K) of the ablated species can be derived to be

$$\begin{aligned} E_K &= 0.25mu^2\cos^2\theta + 1.5kT \\ &\quad + 0.5mu\cos\theta\sqrt{0.25u^2\cos^2\theta + 3kT/m} \\ &= 1.5kT(1 + 0.33M^2\cos^2\theta \\ &\quad + \sqrt{0.05556M^4\cos^4\theta + 0.667M^2\cos^2\theta}). \end{aligned} \tag{9}$$

It is seen that the kinetic energy should decrease in accordance with Eq. (9). In Fig. 7(b), fittings of the measured kinetic energy with Eq. (9) gives the apparent Mach number of 0.52 and 3.0 for Mn^+ and Mn, respectively, also in disagreement with the velocity distributions. Furthermore, the stream velocity of various ablated species does not change with the detection angle in our experiments. We attribute these deviations to the fact that under our experimental condition, the ablated species may obtain stream velocities in all directions rather than only in the target surface normal.

D. Laser fluence effect

Laser fluence has great effects not only on the kinetic energies and relative amount of ablated species, but also on their angular distribution. The dependence of the angular distribution of ablated species on the laser fluence can give some information about the ablation mechanism.[11] Some studies of the angular distribution based on the measurement of the film thickness concluded that the angular distributions of ablated species from metal-oxide targets such as Y-Ba-Cu-O and Sm-Ba-Cu-O are little affected by the laser fluence while the angular distributions of ablated species from polymer targets are much sharper at higher laser fluence. We have measured the angular distribution of laser ablated species from Pr-Sr-Mn-O as a function of the laser fluence at both 355 and 532 nm. Table II lists the bicosine fitting parameters for Mn^+ and Mn as example. It can be seen that when a higher fluence is employed, the sharpness parameter n for the nonthermal component tends to be increased, but the contribution fraction of thermal process seems less sensible to the laser fluence. The mechanism related to the laser fluence effects on the angular distributions may be rather complicated since it depends on the nature of the ablated species as well as the physical properties of the target. However, higher laser fluence will result in higher-ablation yield which enhances the collisions between the ablated species near the surface, it makes the ejection of ablated species more forward peaked. Thus, a greater sharpness parameter n is expected to describe the angular distribution at high fluence.

Besides the laser fluence, other experimental parameters such as the laser beam spot size and incidence angle, the detection distance from the surface, and the ambient pressure, all have significant effects on the angular distributions of ablated species. Furthermore, the effects of laser fluence are also more profound than what we have investigated. Tosnov *et al.* studied the angular distribution of ablated species from Y-Ba-Cu-O and found that a bicosine distribution should be adopted to characterize the angular distribution for a fresh surface, while after some time of irradiation, the thermal component $\cos\theta$ disappeared and only the nonthermal

TABLE II. The bicosine fitting parameter for angular distribution of Mn^+ and Mn and the contribution fraction of thermal process.

Wavelength (nm)	Fluence (J/cm^2)	Mn^+ $a\cos\theta+(1-a)\cos^n\theta$	f	Mn $a\cos\theta+(1-a)\cos^n\theta$	f
355	0.7	$0.17\cos\theta+0.83\cos^{41}\theta$	0.81	$0.26\cos\theta+0.74\cos^{42}\theta$	0.88
355	1.5	$0.21\cos\theta+0.79\cos^{90}\theta$	0.92	$0.25\cos\theta+0.75\cos^{90}\theta$	0.94
355	1.8	$0.10\cos\theta+0.90\cos^{106}\theta$	0.86	$0.28\cos\theta+0.72\cos^{16}\theta$	0.77
532	0.7	$0.23\cos\theta+0.77\cos^{6.6}\theta$	0.53	$0.36\cos\theta+0.64\cos^{6.2}\theta$	0.67
532	1.5	$0.11\cos\theta+0.89\cos^{15}\theta$	0.50	$0.27\cos\theta+0.73\cos^{90}\theta$	0.75
532	1.8	$0.11\cos\theta+0.89\cos^{15}\theta$	0.50	$0.28\cos\theta+0.72\cos^{15}\theta$	0.76

component $\cos^n\theta$ remained in the angular distribution.[20] We have also observed unexpected lump around $\theta=45°$ in some cases as shown in Figs. 3 and 5(a) for PrO^+. Furthermore, even peak ejection shifted away from the surface normal has been also observed. Similar observations have been reported in previous studies,[21,22] but no sound explanation were presented. One reason might be that the local surface is modified after some time of laser irradiation and the local surface normal changes. But we believe that the angular distribution originates in nature from the confinement of the ablated plume expansion by the target surface ($v_z>0$), and minor cones on the surface can not affect the expansion obviously. Foltyn *et al.* have examined this issue carefully, indicating that the presence of cones had not spatially altered the plume.[23] So another reason concerning the incidence direction of laser beam sound more reasonable. When the laser beam irradiates the target surface at an incident angle away from the surface normal, one part of plume away from the laser beam will receive less photons than the other part due to the shielding and thus the resulted plume is not balanced both in density and in temperature. This leads to the distortion in final angular distribution. However, the distorted angular distributions might be related to other mechanisms which depends on the ablation conditions.

IV. CONCLUSIONS

Angular distributions measured with angle- and time-resolved QMS spectrometry for the pulsed laser ablation of a $Pr_{0.67}Sr_{0.33}MnO_3$ target are carried out, and the effects of some ablation parameters on the angular distributions are examined. Our experimental results show that the angular distributions of ablated species usually follow a $\cos^n\theta$ or a bicosine function $a\cos\theta+(1-a)\cos^n\theta$, depending on whether the ejection of the ablated species is attributed to more than one mechanism, i.e., a fast expansion and a slow one. Furthermore, the kinetic energy of neutral ablated species decreases distinctly with increasing the detection angle while that of ionic ablated species seems less depend of the detection angle. Although the laser fluence effects the angular distributions in a completed way, usually a higher directional distribution of the ablated species could be expected for ablation at high-laser fluence. A simple model about the angular distribution is proposed, which can predict the experimental results qualitatively in most cases. However, pulsed laser ablation of multicomponent metal oxides is a complicated process, both the behaviors of the angular distributions of ablated species and their sound explanation need much more endeavor to explore.

*Author to whom correspondence should be addressed. Electronic address: qzqin@fudan.ac.cn

[1] Douglas H. Lowndes, D. B. Geohegan, A. A. Puretzky, D. P. Norton, and C. M. Rouleau, Science **273**, 898 (1996).
[2] G. C. Xiong, S. C. Wu, and D. S. Dai, Sci. China, Ser. A **26**, 722 (1996).
[3] Y. Nishimura, K. Tokunaga, and M. Tsuji, Thin Solid Films **226**, 144 (1993).
[4] Z. Mingfei, F. Zhengwen, Y. Haijun, Z. Zhuangjian, and Q. Qizong, Appl. Surf. Sci. **108**, 399 (1997).
[5] J. P. Zheng, Q. Y. Ying, S. Witanachichi, Z. Q. Huang, D. T. Shaw, and H. S. Kwok, Appl. Phys. Lett. **54**, 954 (1989).
[6] Q. Z. Qin, Z. H. Han, and H. J. Dang, J. Appl. Phys. **83**, 6082 (1998).
[7] H. J. Dang, Z. H. Han, and Q. Z. Qin, Int. J. Mass Spectrom. Ion Processes **178**, 205 (1998).
[8] Z. Fu, M. Zhou, and Q. Qin, Appl. Phys. Lett. **65**, 445 (1997).
[9] H. J. Dang, M. F. Zhou, and Q. Z. Qin, Appl. Spectrosc. **52**, 1154 (1998).
[10] K. Tanaka, T. Miyajima, N. Shirai, Q. Zhuang, and R. Nakata, J. Appl. Phys. **77**, 6581 (1995).
[11] Katherine L. Saenger, *Pulsed Laser Deposition of Thin Films*, edited by Douglas B. Chrisy, and Graham K. Hubler (Wiley, New York, 1994), Chap. 7.
[12] T. Venkatesan, X. D. Wu, A. Inam, and J. B. Wachtman, Appl. Phys. Lett. **52**, 1193 (1988).
[13] T. N. Hansen, J. Schou, and J. G. Lunney, Europhys. Lett. **40**, 441 (1997).
[14] P. Schreiner and H. M. Urbassek, J. Phys. D **30**, 185 (1997).
[15] R. Kelly, J. Chem. Phys. **92**, 5047 (1990).
[16] R. F. Wood, J. N. Leboeuf, D. B. Geohegan, A. A. Puretzky, and K. R. Chen, Phys. Rev. B **58** (3), 1533 (1998).
[17] P. H. Lu and Q. Z. Qin, Sci. China, Ser. A **23** (8), 650 (1993).
[18] Q. Z. Qin, P. H. Lu, Z. J. Zhuang, and Q. K. Zheng, Chem. Phys. Lett. **192**, 265 (1992).
[19] J. C. S. Kools, S. H. Brongersma, E. van de Riet, and J. Dieleman, Appl. Phys. B: Photophys. Laser Chem. **353**, 125 (1991).
[20] R. Tosnov, V. Tsaneva, V. Tsanev, and D. Purounov, J. Low Temp. Phys. **105**, 1307 (1996).
[21] R. P. an Ingen, J. Appl. Phys. **76**, 8065 (1994).
[22] P. K. Schenck, J. W. Hastie, A. J. Paul, and D. W. Bonnell, Proc. SPIE **2403**, 26 (1995).
[23] S. R. Foltyn, R. E. Muenchausen, R. C. Estler, E. Peterson, W. B. Hutcinson, K. C. Ott, N. S. Nogar, K. M. Hubbard, R. C. Dyer, and K. D. Wu, *Laser Abalation for Materials Synthesis*, edited by D. C. Pane and J. C. Bravman MRS Symposium Proceedings No. 191 (Materials Research Society, Pittsburgh, 1990), p. 205.